

# [18] Development of optical flow computation algorithms for strain measurement of solids

Lyubutin P.S.

*Institute of Strength Physics and Materials Science of Siberian Branch of Russian Academy of Sciences, Tomsk Polytechnic University (National Research University)*

## Abstract

This paper deals with development of optical flow algorithms for strain measurement. The aim of the research is to reduce computational efforts and improve robustness of algorithms. Proposed modifications of the algorithms are based on the incremental approach to the estimation of the subsets displacement on the image subsequence, as well as on a three-dimensional recursive search (3DRS). An investigation of robustness and performance of the algorithms shows the advantage of the proposed modifications.

**Keywords:** *DISPLACEMENT VECTOR FIELD, INCREMENTAL APPROACH, IMAGE PROCESSING*

**Citation:** *LYUBUTIN P.S. DEVELOPMENT OF OPTICAL FLOW COMPUTATION ALGORITHMS FOR STRAIN MEASUREMENT OF SOLIDS / LYUBUTIN P.S. // COMPUTER OPTICS. – 2015. – VOL. 39(1). – P. 94-100.*

## Introduction

The term “optical flow” is now widely used in the literature: perceived motions of bright images observed when objects are moving in front of a camera or camera’s motions in stationary environment. Assuming that in normal cases the optical flow doesn’t significantly differ from a motion field, we can evaluate displacements on the time-measured images subsequence. Sufficiently complete overview of various methods to determine the optical flow and their quantitative comparison is given in paper [1], which specifies correlation [2], differential [3-5], phase (frequency) [6] and other approaches.

The optical flow computation algorithms are widely used in different research areas and practical tasks, particularly, to evaluate velocity profiles in liquid- or gas flows using the Particle Image Velocimetry (PIV) method [7], video data compression [8], in transport robotic guidance systems [9].

The Digital Image Correlation (DIC) method is one of the most prospective approaches to study strain and structurally nonuniform materials destruction processes. Its operating principle is to build the displacement vectors based on determination of the optical flow followed by computation of strain components using a numerical differentiation procedure.

When investigating the deformation behavior of structural material patterns using the optical flow computation method [10], one of the main factors limiting the strain evaluation is the increment external load resulting to variance of the surface topography. In case

when the change in the optical surface topography between two images is large enough, it’s not possible to match image subsets. In this regard the use of traditional displacement algorithms becomes unrealizable since there is no opportunity to correctly build the displacement vector field or separate vectors thereon. There are some works well known in this area [11, 12] in which the authors solve similar problems. Thus, in paper [11] two approaches, i.e. the reference-frame approach (RFA) and the incremental difference approach (IDA), have been proposed to search the optical flow.

Not least important is the problem of the algorithm performance. Multi-scale approaches using the image decomposition by Gauss pyramid and enabling to significantly shorten a computation time, have gained widespread acceptance in the image processing and computer vision literature. Approaches based on the use of parallel computations and multiprocessor systems [13-15] are also well known. On the contrary, we know relatively few works dedicated directly to algorithmic optimization of the optical flow computation. In particular, we should note the paper [16] which deals with development of the 3D recursive search (3DRS) method for the block estimation of displacements considering the spatial and temporal relationship of neighboring displacement vectors.

This paper solves the problem of how to increase robustness of the displacement computation algorithm on the images characterized by noticeable changes in the surface topography, as well as opportunities to

use the 3D recursive search (3DRS) algorithm to build the displacement vectors in the task of materials strain evaluation. Comparative studies of robustness of these algorithms were carried out in model and experimental optical image subsequences.

### 1. Algorithm description

The integrated algorithm is supposed to be the basic algorithm, on which modifications proposed in the paper are based. We used the classical correlation procedure in the algorithm to determine pixel accurate displacements [17] and Lucas-Kanade algorithm [4,5] to qualify displacements to pixel bits. This combination is provided, first of all, by good robustness of the correlation algorithm in computation of large displacements, as well as by Lucas-Kanade differential algorithm in computation of displacements with sub-pixel accuracy. Computation of the displacement using the correlation algorithm is based on identifying an extremum of the cross-correlation function of two image subsets. We assume maximum or minimum values as being the extremum depending on the used proximity measure of image subsets. The first case relates to application of the correlation coefficient:

$$ZNCC = \frac{\sum_{i \in B} (F_i - \bar{F})(G_i - \bar{G})}{\sqrt{\sum_{i \in B} (F_i - \bar{F})^2 \sum_{i \in B} (G_i - \bar{G})^2}} \quad (1)$$

where  $F_i$ ,  $G_i$  – are light intensities of two images in point  $i$  of the image subset  $B$ ;  $\bar{F}$ ,  $\bar{G}$  – is the averaging light intensity of subsets. The second case relates to the sum of absolute differences

$$SAD = \sum_{i \in B} |F_i - G_i| \quad (2)$$

Lucas-Kanade algorithm refers to differential optical flow computation algorithms. The algorithm calculates the motion between two images taken at time-points  $t$  and  $t + \delta t$  in each pixel. The differential algorithms are based on the signal approximation by Taylor expansion. Therefore, they use partial derivatives with respect to time- and space coordinates:

$$I(x, y, t) \approx I(x + \delta x, y + \delta y, t + \delta t) \approx I(x, y, t) + \frac{\partial I}{\partial x} \delta x + \frac{\partial I}{\partial y} \delta y + \frac{\partial I}{\partial t} \delta t. \quad (3)$$

Lucas-Kanade algorithm is based on the assumption that in local surroundings of each pixel a value of the optical flow is the same, thus it is possible to record the basic equation of the optical flow for all pixels in the surroundings and to solve the resulting system of equations using the least-square method:

$$\begin{bmatrix} V_x \\ V_y \end{bmatrix} = \begin{bmatrix} \sum_{i \in B} I_{x,i}^2 & \sum_{i \in B} I_{x,i} I_{y,i} \\ \sum_{i \in B} I_{x,i} I_{y,i} & \sum_{i \in B} I_{y,i}^2 \end{bmatrix}^{-1} \begin{bmatrix} -\sum_{i \in B} I_{x,i} I_{t,i} \\ -\sum_{i \in B} I_{y,i} I_{t,i} \end{bmatrix} \quad (4)$$

where  $I_x$ ,  $I_y$ ,  $I_t$  – are partial derivatives of the image light intensity with respect to coordinates  $x$ ,  $y$  and time  $t$ ;  $V_x$ ,  $V_y$  – are the required displacements.

In the process of applying loads to a measurement object the surface topography is formed on its surface, besides the object can be highly strained, extended or compressed. This has resulted in significant differences in images of the object surface in real time if compared to the image of its initial condition. Besides, time-neighboring images in the subsequence may have insignificant changes. In order to eliminate displacement detection errors related to forming the strain surface topography and other processes on the material surface, it has been proposed to evaluate the subsets displacement of neighboring image subsequences with regard to those ones determined for the previous image pairs. This has ensured the possibility to track displacements of the same surface area not only in space, but also in time, that allowed us to improve robustness of displacements computation. The incremental approach has been offered to determine the displacements. A position of the desired subset in the previous image (in regard to the current image subsequence) is identified with the sub-pixel accuracy, so it is necessary to determine light intensity values of pixels in this subset that is carried out using B-spline interpolation.

The classic correlation algorithm enables to compute each coefficient of the cross-correlation function that leads to high computational efforts. Therefore, the further algorithm modification was aimed at reducing computational efforts. For this purpose it was proposed to use the 3-D recursive search (3DRS) method [16]. The 3DRS approach has been widely used in data videostreams processing and it helps to significantly reduce the build time of the displacement vectors field [16]. Each displacement vector is built based on selection of candidate vectors out of the subset using the minimum similarity measure searching procedure for which the sum of absolute differences (SAD) of image segments – current and previous – is used. The method has a probabilistic nature – candidate vectors indicate the assumed direction of the image subsets displacement. The set of candidate vectors includes either time (the given subset displacement vector on the previous image) or spatial components (neighboring vectors), as well as update vectors resulting from spatial displacement vectors (Fig. 1) [16].

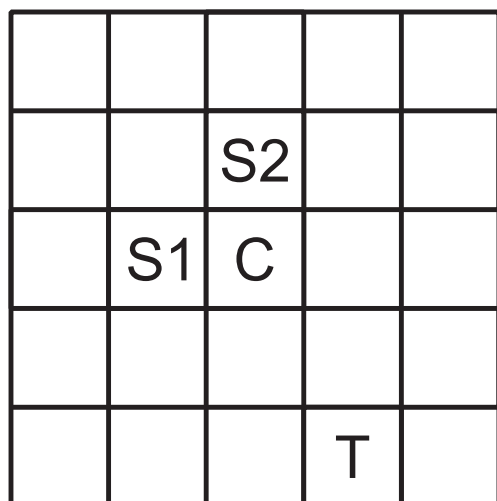


Fig. 1. Arrangement of candidate vectors. *C* - is the displacement vector of the current image area. *S1*, *S2* - are spatial candidate vectors. *T* - is the time candidate vector.

The update vectors are defined as the sum of random vectors throughout a small range (for example,  $-2..2$  in  $x$  and  $y$ -direction) and the displacement vectors determined for the previous adjacent sections *S1* and *S2*. For each of the candidate vectors the similarity measure of the sum of absolute differences (SAD) is computed. The minimum value of the sum of absolute differences (SAD) will define the displacement vector. Thus, the amount of computations of the similarity measure of the sum of absolute differences (SAD) is considerably reduced.

The displacement vector field is computed line-by-line from left to right starting with the top left image subset. When reaching the lower right image subset, the direction of image processing is reversed (right-to-left and bottom-up). So, several passes are performed in this way (usually 5 through 10 passes are set up). The displacement of each subset is confirmed in each subsequent pass including the displacement computed in the previous pass.

With regard to opportunities proposed by the foregoing approaches, we have estimated in this paper the computational efforts and robustness of the displacement vector fields computation for the following algorithms: the incremental algorithm (I); 3DRS with the similarity measure of the sum of absolute differences (SAD) (3DRS); the incremental algorithm with 3DRS (I3DRS).

## 2. Method of testing algorithms

The evaluation of computational costs and robustness of the displacement vectors of the investigated algorithms was performed on model and experimental im-

ages. To estimate errors of the displacement vectors on model images the respective model fields of the displacement vectors have been used.

In the course of experiments, in addition to a form variance in the measurement object surface (compressions, expansions, etc.), the reflecting capacity of its subsets can also change as a result of formation of the strain surface topography and other processes. Material samples, as well as real objects, because of their specific design features, often have stress concentrators (e.g. notches, holes). In the presence of these stress concentrators and in the absence thereof, some cracks can be formed in fragile materials within the field of view, which, in turn, would lead to discontinuity of the displacement field.

The above processes worsen the conditions in which the optical flow computation algorithm performs, and are considered to be constraints in displacements computation. On the basis thereof, the model image subsequences were formed to quantify algorithms robustness.

### Model image subsequences

*Formation of original surface image.* The model image was obtained from a specified number of layers of pseudorandom light intensity references; in this case each layer corresponds to a specific spatial frequency. Similar to the description given in [18], having the initial layer of  $4 \times 4$  pixels after 8 iterations performed, the model image of  $1024 \times 1024$  pixels has been obtained (Fig. 2a).

*Biaxial tension.* In order to simulate variations occurred in the surface when subjected to loadings on biaxial tension, the displacement of each point of the model surface has been assigned (Fig. 2b). For this purpose the light intensity of each pixel of the image is re-computed for the specified strain increment by B-spline interpolation.

*Biaxial tension and surface topography variance (subsequence 1).* To simultaneously register changes related to biaxial tension and surface topography, the subsequence was created where each image was formed from a pair of original images. Computation of image subsequence pixels is carried out as follows:

$$P = (1 - k) \cdot P_1 + k \cdot P_2 \quad (5)$$

where  $P_1$ ,  $P_2$  - are pixel values of original images;  $k$  - is the weighting coefficient varying from 0 to 0.5 with an increment equal to a converse value of the number of images in the subsequence. It results to forming the subsequence consisting of 25 images and reflecting the strain on biaxial tension with the finite increment  $\delta = 80$  pixels.

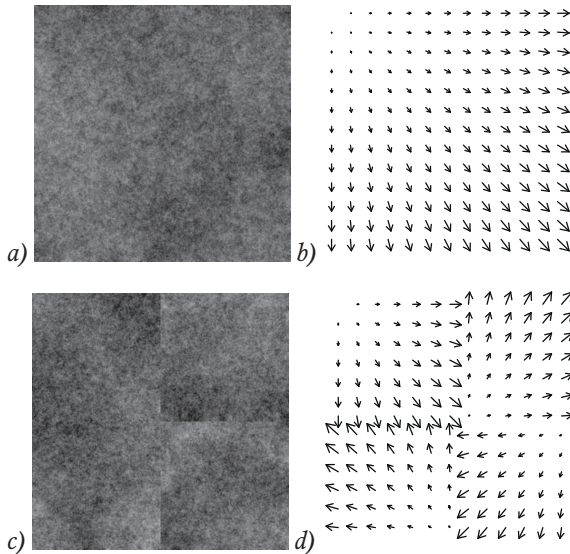


Fig. 2. Model images and displacement vector fields

Images consisting of 4 segments with discontinuity of the displacement vector field (subsequence 2). The analysis of images reflecting the discontinuity of displacements is an important test to identify robustness of the displacement vector fields. For this purpose the biaxial tension of images consisting of 4 segments has been simulated. Each subsequence image was formed from four segments (Fig. 2c) which were composed so as to provide the maximum number of combinations of directions of the displacement vectors at segments' borders (Fig. 2d).

#### Experimental image subsequence

The experimental optical image subsequence was obtained by sample tension from the copper powder sintered in vacuum with an electron beam (Fig. 5a). The specificity of the analyzed images was the significant change in the surface topography when subjected to strain, that imposed special requirements for the displacement vector algorithms. The images were recorded using the foregoing methods described in [19].

#### Evaluation of algorithm performance and robustness

The algorithm performance was evaluated by specific computation time  $t$  of the displacement vector, i.e. a ratio of the total build time of the displacement vectors to the number of vectors herein. To perform computations we used a PC with the following specifications: CPU Intel (R) Core (TM) i3 CPU M 350, RAM 2.00 Gb, OS Windows 7. To investigate the algorithm performance and robustness the above mentioned image subsequences have been used.

To quantify the displacements computation robustness applying the tested algorithms we used the distance field correlation coefficient of vector fields  $K_r$ .

$$K_r = \frac{\sum (D1 - \overline{D1})(D2 - \overline{D2})}{\sqrt{\sum (D1 - \overline{D1})^2 \sum (D2 - \overline{D2})^2}} \quad (6)$$

where  $D1, D2$  – are the field distances of respective vector fields which are required for transition from two component vector field data to single component data;  $\overline{D1}, \overline{D2}$  – are the arithmetic mean values of respective distance fields. Each element of the distance field was determined as follows [20]:

$$D_{ij} = \sum_{k=1}^w \sum_{l=1}^h (|x_{ij} - x_{kl}| + |y_{ij} - y_{kl}|), i=1..w, j=1..h \quad (7)$$

where  $x, y$  – are respective vector components;  $w, h$  – are width and height of the displacement vector field.

### 3. Test results

#### Testing on model images

The analysis of computation time of one displacement vector has shown the value  $t$  to be maintained approximately at a constant level for all algorithms, regardless of the value of variable parameters for all investigated model image subsequences.

In all observed image subsequences the minimum  $t$  value has been recorded for 3DRS and I3DRS algorithms which is  $\sim 10$  times less than for the incremental I algorithm (Fig. 3a). The dependence of computation time of the complete displacement vector field from the number of vectors in  $N_v$  shown in Fig. 3b is linear. The ratio of execution time of incremental I and 3DRS (I3DRS) algorithms is maintained regardless of the number of vectors in the field.

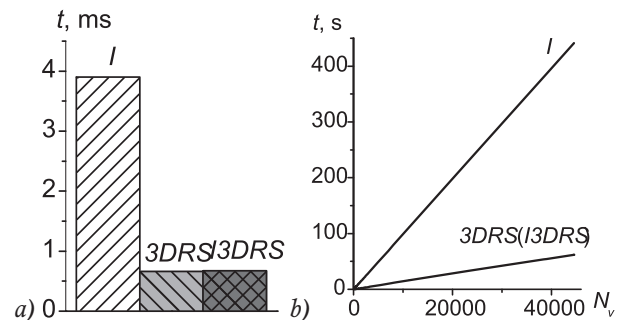


Fig. 3. Dependence of computation time of one vector (a) and computation time of the complete displacement vector field from the number of vectors (b) for incremental I, 3DRS, I3DRS algorithms

To quantify the displacements computation robustness applying the tested algorithms we used the displacement vector fields built while processing the model image subsequences. For this purpose we computed  $K_r$  (6), just as described in the previous section (Fig. 4).

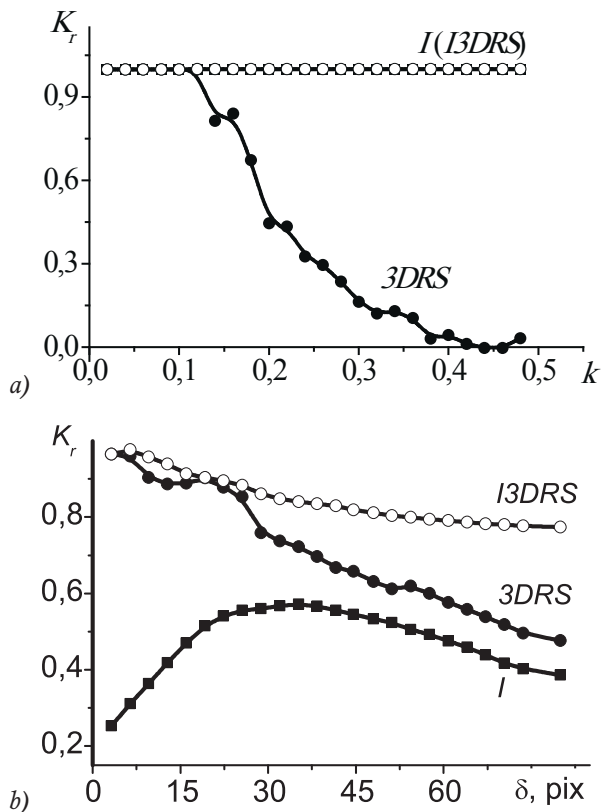


Fig. 4. Dependence of the correlation coefficient of vector fields from the weighting coefficient (subsequence 1) (a), the biaxial strain increment of fragmented images (subsequence 2) (b) for incremental I, 3DRS, I3DRS algorithms

The graph of changing  $K_r$  from the “weighting coefficient”  $k$  (5) for subsequence 1 is shown in Fig. 4a. It can be seen that the 3DRS algorithm, which is not based on the incremental approach, doesn't allow to accurately build the complete displacement vector field: for 3DRS  $K_r$  value is to be reduced when  $k > 0.1$ . This is due to the inability to set up a corresponding image area. At the same time, incremental algorithms (I, I3DRS) show that  $K_r$  value is close to unity.

Reduced  $K_r$  is typical for all algorithms when tested on subsequence 2 (Fig. 4b). Low  $K_r$  values at the beginning of the subsequence for the incremental algorithm are related to the presence of incorrectly built displacement vectors, which are much greater in absolute terms than the mean length of the vectors correctly identified throughout the displacement vector field; the number of false and correct displacement vectors becomes approximately equal by the middle of the subsequence. The total reduction of  $K_r$  for all algorithms relates to the increase of displacement values along the segments' borders (discontinuities of the displacement field). Thus, the best robustness has been shown by I3DRS algorithms.

### Testing on experimental images

Results of the study of algorithms on the experimental image subsequence (Fig. 5 a, b) revealed that for algorithms 3DRS and I3DRS the computation time  $t$  is less in its value than that one for the incremental algorithm. To compare robustness of the algorithms (Fig. 5c) the results obtained using the I3DRS algorithm have been considered as the “true” displacement vector fields (based on results of algorithms testing on model images).

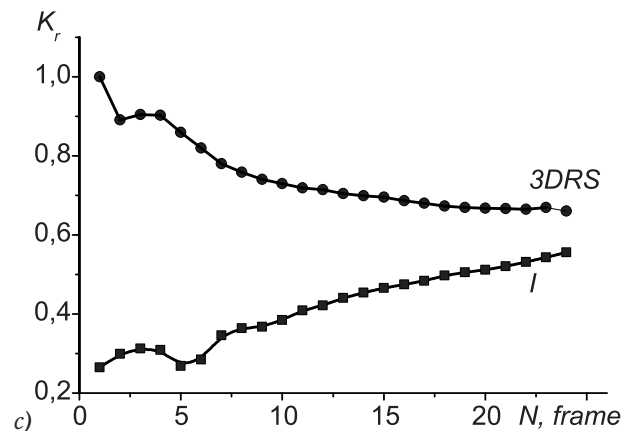
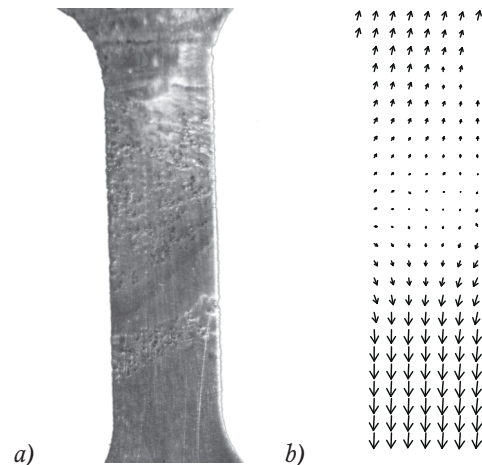


Fig. 5. Optical image of the sample (a) and the displacement vector field (b) obtained from experimental images; dependence of  $K_r$  on the image number (strain degree) for incremental I and 3DRS algorithms based on processing results of experimental image subsequences (c)

It is obvious that the incremental algorithm may significantly concede the 3DRS algorithm, and the increased  $K_r$  is similar to that one valid for this algorithm in the model subsequence 2 (Fig. 5c). The 3DRS algorithm graph has also the same pattern of change, which is similar for this algorithm in the model subsequence 2 (Fig. 5c): a gradual decline of  $K_r$  can be observed with increasing the variable parameter. Thus, results of algorithms testing on experimental and model images correlate well.

## Conclusion

The paper offers the algorithm to build displacement vector fields based on the incremental approach to the estimation of the subsets displacement on the image subsequence. The paper also offers the modification of the incremental algorithm based on the 3DRS approach. Comparative studies on model and experimental data have been performed, which showed that the developed algorithm performs well when evaluating the displacements on the material surface in conditions of considerable strain increments. In contrast to the classical correlation algorithm, in which the displacement evaluation is made without regard to changes on the material surface, the proposed algorithm possesses adequate robustness to evaluate displacements throughout the full range of the strain increment.

The application efficiency of the 3DRS approach has been identified with regard to reducing computation efforts. In this case, the time required for the algorithm I3DRS to build the displacement vector field is 10 times less if compared to the execution time of the incremental algorithm I.

Therefore, among all test combinations a combination of incremental and 3DRS approaches is the best one both in computational efforts and robustness to identify the displacement fields in the optical strain evaluation method. The latter – 3DRS – approach enables to significantly reduce computational efforts and to simultaneously increase robustness in the displacement vectors if compared to application of the incremental and 3DRS algorithms separately.

## Acknowledges

The work has been performed with partial support of the Fundamental Studies Program of the National Academies of Sciences for 2013-2020, the RFBR (the Russian Foundation for Basic Researches) grant No. 13-07-00009 and the grant No. SP-816.2012.5.

## References

1. **Barron, J.L.** Performance of optical flow techniques / J.L. Barron, D.J. Fleet, S.S. Beauchemin // *International Journal of Computer Vision*. – 1994. – Vol. 12. – P. 43-77.
2. **Sutton, M.A.** Image correlation for shape, motion and deformation measurements: basic concepts, theory and applications / M.A. Sutton, J.-J. Orteu, H. Schreier. – Springer. – 2009. – P. 321.
3. **Horn, B.K.P.** Determining optical flow / B.K.P. Horn, B.G. Schunck // *Artificial Intelligence*. – 1981. – Vol. 17. – P. 185-203.
4. **Lucas, B.D.** An iterative image registration technique with an application to stereo vision / B.D. Lucas, T. Kanade // *Proceedings of the 7th international joint conference on Artificial intelligence*. – 1981. – Vol. 2. – P. 674-679.
5. **Lucas, B.D.** Generalized Image Matching by the Method of Differences / B.D. Lucas. – doctoral dissertation, tech. report. – Robotics Institute, Carnegie Mellon University, July, 1984. – P. 167.
6. **Fleet, D.J.** Phase-based disparity measurement / D.J. Fleet, A.D. Jepson, M.R.M. Jenkin // *CVGIP: Image Understanding*. – 1991. – Vol. 53. – P. 198-210.
7. **Raffel, M.** Particle Image Velocimetry: A Practical Guide 2nd ed. / M. Raffel, C.E. Willert, S.T. Wereley, J. Kompenhans. – Springer, Berlin. – 2007. – P. 448.
8. **Belyaev, E.A.** Motion estimation algorithms for low bit-rate video compression / E.A. Belyaev, A.M. Turlikov // *Computer Optics*. – 2008. – Vol. 32(4). – P. 403-412. (In Russian).
9. **Giachetti, A.** The use of optical flow for road navigation / A. Giachetti, M. Campani, V. Torre // *IEEE Transactions on Robotics and Automation*. – 1998. – Vol. 14(1). – P. 34-48.
10. **Syryamkin, V.I.** Television-optical technique for materials investigation and diagnostics of state of loaded materials and structure parts / V.I. Syryamkin, S.V. Panin // *Computational technologies*. – 2003. – Vol. 8. – Special issue. – P. 10-25. (In Russian).
11. **Wang, C.-M.** Estimating Optical Flow by Integrating Multi-Frame Information / C.-M. Wang, K.-C. Fan, C.-T. Wang // *Journal of Information Science and Engineering*. – 2008. – Vol. 24(6). – P. 1719-1731.
12. **Irani, M.** Multi-Frame Optical Flow Estimation Using Subspace Constraints / M. Irani // *Seventh International Conference on Computer Vision (ICCV'99)*. – 1999. – Vol. 1. – P. 626-633.
13. **Tao, M.** Simple Flow: A Non-iterative, Sublinear Optical Flow Algorithm / M. Tao, J. Bai, P. Kohli, S. Paris // *Computer Graphics Forum*. – May 2012. – Vol. 31(2/1). – P. 345-353.
14. **Marzat, J.** Real-time dense and accurate parallel optical flow using CUDA / J. Marzat, Y. Dumortier, A. Ducrot // *Proc. 7th Int'l Conf. in Central Europe on Computer Graphics, Visualization and Computer Vision (WSCG)*. – 2-5 Feb. 2009. – P. 105-111.
15. **Durkovic, M.** Performance of Optical Flow Techniques on Graphics Hardware / M. Durkovic, M. Zwick, F. Obermeier, K. Diepold // *IEEE International Conference on Multimedia and Expo*. – 2006. – P. 241-244.
16. **Braspenning, R.A.** True-motion estimation using feature correspondence / R.A. Braspenning, G. de Haan // *SPIE, Proceedings of Visual Communications and Image Processing*. – Jan. 2004. – Vol. 5308. – P. 396-407.
17. **Lyubutin P.S.** Investigation of accuracy and error rate performance of the displacement vector construction in evaluation of strains using TV-optical technique / P.S. Lyubutin, S.V. Panin // *Computational technologies*. – 2006. – Vol. 11(2). – P. 52-66. (In Russian).
18. **Panin, S.V.** Application of the fractal dimension for estimating surface images obtained by various detectors / S.V. Panin, Yu.A. Altukhov, P.S. Lyubutin, A.V. Byakov, S.A. Khizhnyak // *Optoelectronics, Instrumentation and Data Processing*. – 2013. – Vol. 49(1). – P. 34-40.
19. **Panin, S.V.** Study of Deformation and Fracture Using Data of Acoustic Emission, Correlation of Digital Images and Strain-Gauging / S.V. Panin, A.V. Byakov, P.S. Lyubutin, O.V.

Bashkov, V.V. Grenke, I.V. Shakirov, S.A. Khizhnyak // Industrial Laboratory. – 2011. – Vol. 77(9). – P. 50-59.

■ **20. Voskoboynikov, Yu.E.** Nonlinear algorithms for vector signal filtering / Yu.E. Voskoboynikov, V.G. Belyavtsev // Optoelectronics, Instrumentation and Data Processing. – 1999. – Vol. 35(5). – P.29-38.

